Nucleus Segmentation in Histology Images with Hierarchical Multilevel Thresholding

Hady Ahmady Phoulady[a], Dmitry B. Goldgof[a], Lawrence O. Hall[a], and Peter R. Mouton[b]

[a]Department of Computer Science and Engineering, University of South Florida, Tampa, FL, USA

[b]Department of Pathology and Cell Biology, University of South Florida, Tampa, FL, USA

ABSTRACT

Automatic segmentation of histological images is an important step for increasing throughput while maintaining high accuracy, avoiding variation from subjective bias, and reducing the costs for diagnosing human illnesses such as cancer and Alzheimer's disease. In this paper, we present a novel method for unsupervised segmentation of cell nuclei in stained histology tissue. Following an initial preprocessing step involving color deconvolution and image reconstruction, the segmentation step consists of multilevel thresholding and a series of morphological operations. The only parameter required for the method is the minimum region size, which is set according to the resolution of the image. Hence, the proposed method requires no training sets or parameter learning. Because the algorithm requires no assumptions or a priori information with regard to cell morphology, the automatic approach is generalizable across a wide range of tissues. Evaluation across a dataset consisting of diverse tissues, including breast, liver, gastric mucosa and bone marrow, shows superior performance over four other recent methods on the same dataset in terms of F-measure with precision and recall of 0.929 and 0.886, respectively.

Keywords: nucleus segmentation, histology, multilevel thresholding, color deconvolution, morphological operations

1. INTRODUCTION

Cellular features such as nuclear size, distribution and texture play an important role in diagnosis and grading of diseases from histology tissue. To automatically quantify features of microscopic nuclei in images of stained tissue, nuclei locations and boundaries must first be located. Nuclei detection and segmentation has been addressed with a variety of algorithms, including Gaussian mixture clustering,[1] gradient flow tracking,[2] watershed[3] and graph cuts.[4] Color normalization and color deconvolution can be used to take advantage of color information from different stains to enhance results of nuclear segmentation.[5] However, a general approach has been elusive because nuclei can be clustered and exhibit a range of shapes, sizes, and colors depending on staining method and tissue type.[6] In this paper, we propose a general algorithm for segmenting nuclei stained with hematoxylin and eosin (H&E) and evaluate the performance using a dataset of biopsy images from various tissues. The proposed method requires no parameter learning or training data because the parameter values are set adaptively, making the approach insensitive to variations in staining intensity. The Matlab code of the proposed method will be made available publicly to enable further research and benchmarking*.

2. MATERIALS AND METHOD

The dataset used to evaluate the proposed method was provided by Wienert et al.,[7] and is discussed in the following Subsection.

Further author information: (Send correspondence to H.A.P.)
H.A.P.: E-mail: hady@mail.usf.edu
D.B.G.: E-mail: goldgof@mail.usf.edu
L.O.H.: E-mail: lohall@mail.usf.edu
P.R.M.: E-mail: pmouton@health.usf.edu

*The Matlab code can be downloaded at http://www.csee.usf.edu/~hady/codes/2016SPIE_histology_segmentation.zip.

Medical Imaging 2016: Digital Pathology, edited by Metin N. Gurcan, Anant Madabhushi, Proc. of SPIE Vol. 9791, 979111 · © 2016 SPIE
CCC code: 1605-7422/16/$18 · doi: 10.1117/12.2216632

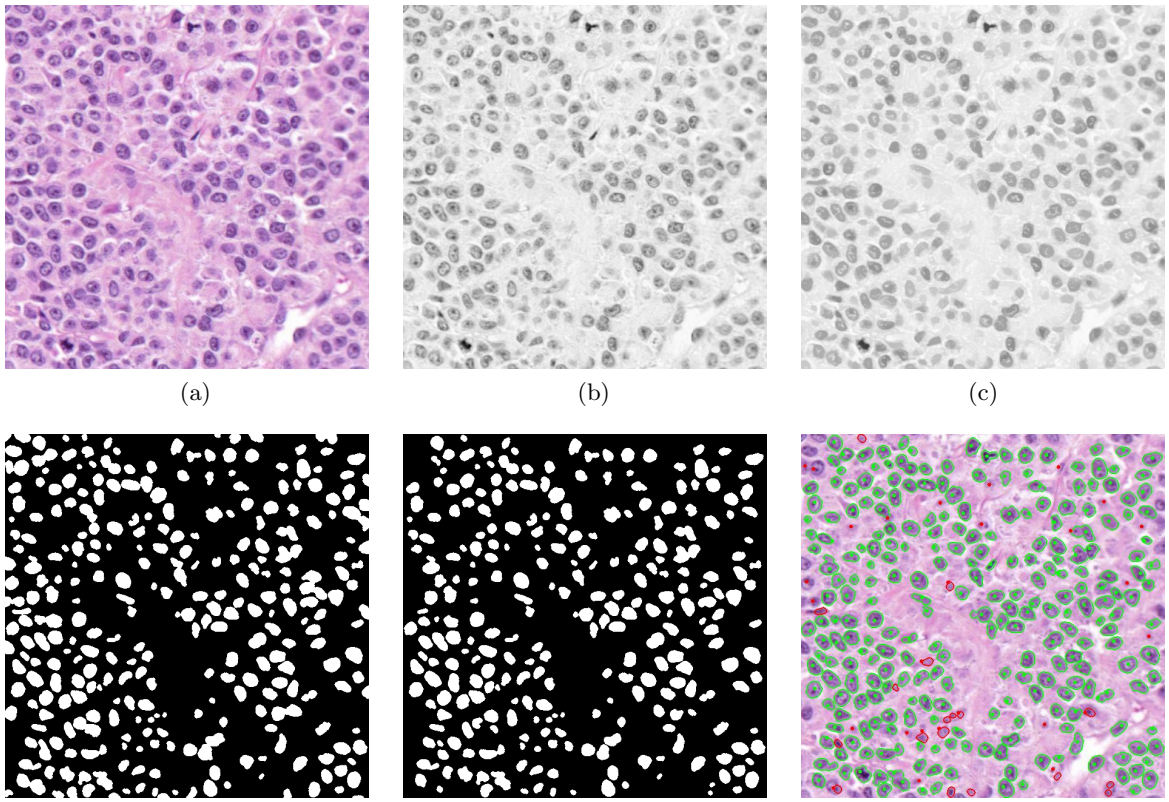

Figure 1: Flow of hierarchal multilevel thresholding approach: (a) Original image, (b) Hematoxylin channel after color deconvolution, (c) Opening by reconstruction on hematoxylin channel, (d) The first binarization followed by morphological operations, (e) The result after a series of binarizations, morphological operations, region splitting and removing boundary regions, (f) The contours on the original image - green dots, red dots and red contours are true positives, false negatives and false positives respectively.

2.1 Gold Standard Dataset

The limited number of public datasets for histopathology analysis increases the difficulty of comparing different methods. This dataset includes a wide variety of tissues such as breast cancer samples representing a broad morphological variety, including normal tissue components; bone marrow with normal and pathologically altered cells; normal liver tissue; kidney tissue; and intestinal mucosa.[7] The dataset consists of thirty-six histology images (600x600 pixels each) with ground truth. The dataset includes a total of 7931 consistently labeled cells by consensus agreement of three pathologists.

2.2 Overview of the Method

Steps of the method are divided into two main parts: preprocessing and segmentation. The preprocessing step consists of color deconvolution and image reconstruction. Segmentation is based on binarization of the image from a threshold obtained from a multilevel thresholding algorithm. The resulting segmentation divides "large" regions into smaller regions followed by morphological operations to separate close regions and smooth out the boundaries. The flow of our approach is presented in Fig. 1.

2.3 Preprocessing

The preprocessing step includes color deconvolution[8] by modeling the image colors based on the Beer-Lambert Law. Since hematoxylin stains nucleic acids in the cell nucleus, the hematoxylin channel was used for nuclear

segmentation. The resulting grayscale image was then processed with opening by reconstruction to connect close background regions to each other.

We do not performed closing by reconstruction, a common process after opening by reconstruction. Due to low resolution of images, closing by reconstruction connects some adjacent nuclei to each other and therefore segments them as a single nucleus. The processed image was then ready for segmentation.

2.4 Automated Threshold Selection

The next step was to iteratively binarize the preprocessed grayscale image and form the regions as nuclei. Selection of thresholds for this step was done using 1 through 10-level (multilevel) thresholding based on the Otsu method,[9] as described by Liao et al.[10] Each of these multilevel thresholdings divides the pixel intensities to (level + 1) classes with minimal combined intra-class variance and equivalently maximal inter-class variance.[9] We retained the lowest thresholds of each multilevel thresholding, a total of up to 10 different thresholds that specified the darkest class in the image in each corresponding multilevel thresholding. After a descending sort on this set of thresholds, the image was binarized from the highest threshold. The first formed regions were considered as initial regions and each subsequent binarization produces a subset of (usually smaller) regions from a previous binarization. This process may cause division of some regions into two or more regions; in this case, the new (smaller) regions replaced the larger region. If a region was simply shrunk in a new binarization, however, that region was not replaced. Each initial region may be therefore replaced later only if it split into two or more regions.

After each binarization, an opening operation was performed to separate weakly connected regions. Holes in the regions were filled to reconstruct the regions with holes mostly obtained from cancer cells. Regions smaller than a predefined size, m, were removed to eliminate the segmented of tissue artifacts. Finally, regions connected to the boundary of an image were removed.

Because of the preprocessing step, segmented region boundaries were usually formed inside the nuclei area. Therefore, the final nuclei outlines were obtained by dilating the final regions with a disk of radius one pixel, giving a more visually accurate approximation of the boundaries.

3. RESULTS

The single parameter in the method, m, specifies the size of the smallest permitted region. In the present study, m is set to 50 pixels as in the study by Wienert et al.[7] that supplied our images. The structuring elements for opening by reconstruction and opening to separate weakly connected regions are set to a disk with radius three pixels based on the image size. Choosing a disk with radius two or four pixels affects the results by about one percent. The goal in selecting structuring elements with radius three pixels is to avoid: 1) a too large structuring element that removes important detail in the image; and 2) a too small structuring element that fails to connect close background parts to each other, which could degrade the results more than a couple percent. Increasing the number of levels when choosing the thresholds changes the computation time but does not significantly change the results.

True positive (TP) is defined as the number of manual points in ground truth that fall inside the segmented nuclei. False positive (FP) is the number of segmented nuclei that include no manual points. False negative (FN) is the number of manual labeled points that do not fall into any segmented nucleus. The results are presented in terms of precision, recall, F-measure and conglomerate, which are described in the following.

Precision, recall and F-measure are computed as below:

$$\text{Precision} = \frac{\text{TP}}{\text{TP} + \text{FP}},\ \text{Recall} = \frac{\text{TP}}{\text{TP} + \text{FN}} \text{ and F-measure} = 2 \cdot \frac{\text{Precision} \cdot \text{Recall}}{\text{Precision} + \text{Recall}}.$$

Lastly, conglomerate is defined as

$$\text{Conglomerate} = \frac{\text{N} - \text{FP}}{\text{TP}},$$

where N is the number of segmented regions.

For comparison, we include the results of the proposed method along with four other sets of results. The first two sets of results are from a method[4] proposed by Al Kofahi et al., with two versions of "automatic" and "optimized", which uses nine parameters. The other two sets of results are from methods proposed by Wienert et al.,[7] which use five parameters and Veta et al.,[3] which uses a fixed set of structuring elements and three parameters which need to be trained and are mainly used to select the best candidates for the final contours. A summary of the results is presented in Table 1[†].

Table 1: Results summary - superior results are shown with bold font.

	Precision	Recall	F-measure	Conglomerate
Al Kofahi (automatic)[4]	0.717	**0.908**	0.801	0.964
Al Kofahi (optimized)	0.823	**0.908**	0.863	0.966
Wienert[7]	0.908	0.859	0.883	0.958
Veta[3]	0.904	0.833	0.867	**0.989**
Proposed Method	**0.929**	0.886	**0.907**	0.952

4. DISCUSSION

The proposed method achieves the highest precision measure and its recall measure is very near the highest value among all methods. Hence, our approach has the highest F-measure. The conglomerate measure is the lowest but comparable to first three methods. Thus, the proposed method tends to segment overlapped (or touching) nuclei to a greater extent than the other methods. This result is expected since the regions are segmented by multilevel thresholding and, in this process, miss a low intensity difference between two close nuclei. The under-segmentation of the overlapped nuclei can be potentially handled by an additional post-processing step. For example, because a region that is segmenting overlapped nuclei usually has a low solidity (ratio of the region's area to the area of its convex hull), to improve the conglomerate score in post-processing we can simply remove all segmented regions with solidity less than 0.8. With this step, the approach achieves a precision, recall, F-measure and conglomerate of 0.930, 0.860, 0.894 and 0.959, respectively. However, to achieve a high conglomerate measure as with the method proposed by Veta et al., and at the same time keep a good value of precision and recall, a more advanced post-processing step is required.

The algorithm is insensitive to minor parameter changes as evidenced by only a few percent changes in the results by modifications such as performing closing by reconstruction after opening by reconstruction in preprocessing; imposing a largest region's area limit during binarization; increasing the minimum permitted region's area; and using morphological features such as solidity and boundary saliency to reject some regions.

In terms of speed, the whole process, including color deconvolution, preprocessing, segmentation and computing different measures takes on average about one second (1.02) for each image on a PC with 2.4 GHz CPU.

Four examples of segmentation results of different tissues are presented in Fig. 2.

5. CONCLUSIONS AND FUTURE WORK

An algorithm is proposed to segment nuclei in histology images stained with H&E, a general stain in pathology for evaluating a wide range of normal and diseased tissue. Using color deconvolution, image reconstructions, iterative multilevel thresholding and morphological operations, our approach segments nuclei in a wide variety of histology images from various tissue types. The algorithm requires a single parameter for specifying the smallest permitted region area during the process of removing regions. The results show high precision and recall on

[†]The results of the method proposed by Al Kofahi et al. are taken from Ref. 7. Also, the F-measure values are computed based on the corresponding precision and recall.

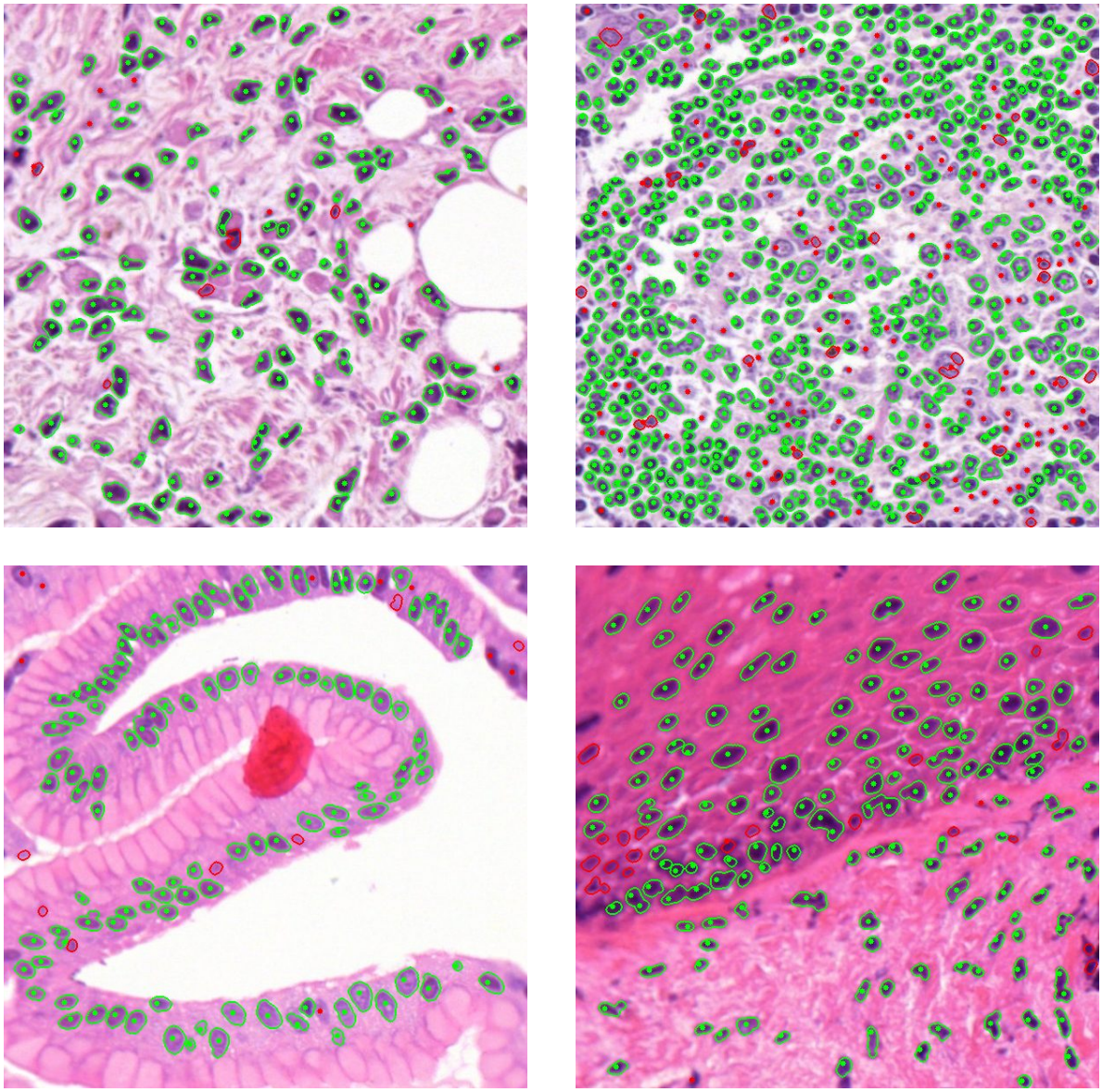

Figure 2: Segmentation results of four images in dataset - green dots, red dots and red contours are true positives, false negatives and false positives respectively.

a dataset including normal and cancerous tissues of different types, and superior performance in terms of F-measure (with precision 0.929 and recall 0.886) as compared to other reported results on the same dataset. For future work, post-processing steps can be designed to separate clumped nuclei and refine the boundaries. Since many missed manual points lie very close to the boundaries of segmented regions and clumped nuclei, these can be effectively found by checking features such as solidity of the segmented regions. These additional steps can potentially increase the conglomerate measure while improving precision and recall measures.

ACKNOWLEDGMENTS

This research supported by grants to P.R.M. from the Florida High Technology Corridor (Heathrow, FL), the USF Health Byrd Alzheimer Institute (Tampa, FL), and the Stereology Research Center (Tampa,-St. Petersburg, FL).

REFERENCES

[1] Fatakdawala, H., Xu, J., Basavanhally, A., Bhanot, G., Ganesan, S., Feldman, M., Tomaszewski, J. E., and Madabhushi, A., "Expectation maximization-driven geodesic active contour with overlap resolution (emagacor): Application to lymphocyte segmentation on breast cancer histopathology," *Biomedical Engineering, IEEE Transactions on* **57**, 1676–1689 (July 2010).

[2] Huang, P.-W. and Lai, Y.-H., "Effective segmentation and classification for hcc biopsy images," *Pattern Recognition* **43**(4), 1550 – 1563 (2010).

[3] Veta, M., van Diest, P. J., Kornegoor, R., Huisman, A., Viergever, M. A., and Pluim, J. P. W., "Automatic nuclei segmentation in h&e stained breast cancer histopathology images," *PloS one* **8**(7), e70221 (2013).

[4] Al-Kofahi, Y., Lassoued, W., Lee, W., and Roysam, B., "Improved automatic detection and segmentation of cell nuclei in histopathology images," *Biomedical Engineering, IEEE Transactions on* **57**, 841–852 (April 2010).

[5] Khan, A. M., Rajpoot, N., Treanor, D., and Magee, D., "A nonlinear mapping approach to stain normalization in digital histopathology images using image-specific color deconvolution," *Biomedical Engineering, IEEE Transactions on* **61**, 1729–1738 (June 2014).

[6] McCann, M. T., Ozolek, J. A., Castro, C. A., Parvin, B., and Kovacevic, J., "Automated histology analysis: Opportunities for signal processing," *Signal Processing Magazine, IEEE* **32**, 78–87 (Jan 2015).

[7] Wienert, S., Heim, D., Saeger, K., Stenzinger, A., Beil, M., Hufnagl, P., Dietel, M., Denkert, C., and Klauschen, F., "Detection and segmentation of cell nuclei in virtual microscopy images: A minimum-model approach," *Scientific Reports* **2**, 503 (2012).

[8] Ruifrok, A. C. and Johnston, D. A., "Quantification of histochemical staining by color deconvolution," *Analytical and quantitative cytology and histology / the International Academy of Cytology [and] American Society of Cytology* **23**(4), 291–9 (2001).

[9] Otsu, N., "A threshold selection method from gray-level histograms," *Systems, Man and Cybernetics, IEEE Transactions on* **9**, 62–66 (Jan 1979).

[10] Liao, P.-S., Chen, T.-S., and Chung, P.-C., "A fast algorithm for multilevel thresholding," *Journal of Information Science and Engineering* **17**, 713–727 (2001).